A peer-reviewed version of this preprint was published in PeerJ on 19 April 2019.

Goode AG, Fields DM, Archer SD, Martínez Martínez J. 2019. Physiological responses of *Oxyrrhis marina* to a diet of virally infected *Emiliania huxleyi*. PeerJ 7:e6722 https://doi.org/10.7717/peerj.6722

Physiological responses of *Oxyrrhis marina* to a diet of virally infected *Emiliania huxleyi*

Andrew G Goode [1, 2] , **David M Fields** [1] , **Stephen D Archer** [1] , **Joaquín Martínez Martínez** Corresp. [1]

[1] Bigelow Laboratory for Ocean Sciences, East Boothbay, Maine, United States
[2] School of Marine Sciences, University of Maine, Orono, Maine, United States

Corresponding Author: Joaquín Martínez Martínez
Email address: jmartinez@bigelow.org

The coccolithophore *Emiliania huxleyi* forms some of the largest phytoplankton blooms in the ocean. The rapid demise of these blooms has been linked to viral infections. *E. huxleyi* abundance, distribution, and nutritional status make them an important food source for the heterotrophic protists which are classified as microzooplankton in marine food webs. In this study we investigated the fate of *E. huxleyi* (CCMP 374) infected with virus strain EhV-86 in a simple predator-prey interaction. The ingestion rates of *Oxyrrhis marina* were significantly lower (between 26.9 and 50.4%) when fed virus-infected *E. huxleyi* cells compared to non-infected cells. Despite the lower ingestion rates, *O. marina* showed significantly higher growth rates (between 30 and 91.3%) when fed infected *E. huxleyi* cells, suggesting higher nutritional value and/or greater assimilation of infected *E. huxleyi* cells. No significant differences were found in *O. marina* cell volumes or fatty acids profiles. These results show that virally infected *E. huxleyi* support higher growth rates of single celled heterotrophs and in addition to the “viral shunt” hypothesis, viral infections may also divert more carbon to mesozooplankton grazers.

Physiological responses of *Oxyrrhis marina* to a diet of virally infected *Emiliania huxleyi*

Andrew G. Goode[1,2], David M. Fields[1], Stephen D. Archer[1], Joaquín Martínez Martínez[1]*

[1]Bigelow Laboratory for Ocean Sciences, East Boothbay, ME, USA 04544

[2]University of Maine, School of Marine Sciences, Orono, ME, USA 04469

*Corresponding Author. Joaquín Martínez Martínez, email: jmartinez@bigelow.org

Running Title: *O. marina* response to infected prey

Key Words: phytoplankton, zooplankton, coccolithophore, dinoflagellate, *Emiliania huxleyi*, *Oxyrrhis marina*, virus, carbon, grazing, growth, fatty acids, food web

Abstract:

The coccolithophore *Emiliania huxleyi* forms some of the largest phytoplankton blooms in the ocean. The rapid demise of these blooms has been linked to viral infections. *E. huxleyi* abundance, distribution, and nutritional status make them an important food source for the heterotrophic protists which are classified as microzooplankton in marine food webs. In this study we investigated the fate of *E. huxleyi* (CCMP 374) infected with virus strain EhV-86 in a simple predator-prey interaction. The ingestion rates of *Oxyrrhis marina* were significantly lower (between 26.9 and 50.4%) when fed virus-infected *E. huxleyi* cells compared to non-infected cells. Despite the lower ingestion rates, *O. marina* showed significantly higher growth rates (between 30 and 91.3%) when fed infected *E. huxleyi* cells, suggesting higher nutritional value and/or greater assimilation of infected *E. huxleyi* cells. No significant differences were found in *O. marina* cell volumes or fatty acids profiles. These results show that virally infected *E. huxleyi* support higher growth rates of single celled heterotrophs and in addition to the "viral shunt" hypothesis, viral infections may also divert more carbon to mesozooplankton grazers.

INTRODUCTION

Cell lysis, due to viral infection, accounts for up to 30% of daily mortality rates of marine microorganisms (Suttle 1994; van Hannen et al. 1999), influences shifts in microbial community structure (Martínez Martínez et al. 2006; Thingstad 2000), and is hypothesized to result in the reduction of net primary productivity (Suttle 1994). Conventional dogma holds that virus-induced cell lysis can divert energy away from the traditional food web by releasing the organic carbon (C), nitrogen (N), and phosphorus (P) in phytoplankton cells to the dissolved phase, fueling an active bacterial population. This process, known as the "viral shunt", is hypothesized to transfer 6 – 26% of C (estimated 150 gigatons of C per year) from photosynthetic plankton to the dissolved organic pool (Suttle 2005; Wilhelm & Suttle 1999). However, to the best of our knowledge, the magnitude of the C "shunt" during viral infection has not been directly measured. A quantitative understanding of the pathways and factors that affect the flow of organic C in marine systems is key to understanding community structure and for predicting resource availability to support important commercial species. Although it is known that viral infection of algal cells alters crucial cellular and biogeochemical processes (Evans et al. 2009; Gilg et al. 2016; Malitsky et al. 2016; Rosenwasser et al. 2014; Suzuki & Suzuki 2006), the impacts of these changes on the nutritional value of cells and on the grazing and growth rates of both micro- and macrozooplankton are largely unexplored (Evans & Wilson 2008; Vermont et al. 2016).

The coccolithophore *Emiliania huxleyi* is a globally distributed and abundant oceanic phytoplankton species whose blooms can cover thousands of square kilometers (Holligan et al. 1993). They are a key component in pelagic food webs contributing essential amino acids and fatty acids (FA) to the base of the food chain, which are crucial for supporting multiple cellular functions and growth in higher trophic level organisms. The collapse of *E. huxleyi* blooms have

been linked to infection by double-stranded (ds) DNA viruses (EhVs) (Bratbak et al. 1993; Brussaard et al. 1996; Wilson et al. 2002). Infection with EhV causes rapid physiological changes in *E. huxleyi* that divert host resources toward virus replication and assembly; e.g., decreased photochemical efficiency (Gilg et al. 2016) and altered metabolic pathways such as glycolysis, FA, and nucleotide biosynthesis (Evans et al. 2009; Malitsky et al. 2016; Rosenwasser et al. 2014). Within three hours post inoculation with EhV, infected cultures shift from producing polyunsaturated (PUFA) to monounsaturated (MUFA) and saturated (SFA) fatty acids relative to non-infected cultures (Floge 2014). Additionally, viral infection can increase the uptake capacity of N and P by expressing viral genes which code for nutrient transporters not found in the host's genome and increase access to diverse nutrient sources unavailable to uninfected cells (Monier et al. 2017; Monier et al. 2012; Wilson et al. 1996). High P and/or N resources are critical for optimal viral proliferation in phytoplankton hosts (Maat & Brussaard 2016; Maat et al. 2016; Mojica & Brussaard 2014; Monier et al. 2017), including *E. huxleyi* (Bratbak et al. 1993; Martínez Martínez 2006) At the scale of large oceanic *E. huxleyi* blooms it remains unclear if the sum of viral alterations enhance or diminish the overall amount of C and essential nutrients that are passed to higher trophic levels.

Predation by heterotrophic and mixotrophic protists (microzooplankton) dominates grazing on phytoplankton in aquatic microbial food webs, and plays a key role in C cycling and nutrient regeneration (Sherr & Sherr 2002; Sherr & Sherr 2009). The heterotrophic dinoflagellate *Oxyrrhis marina* has been shown to preferentially graze on EhV-infected *E. huxleyi* cells, relative to uninfected cells (Evans & Wilson 2008). Although the mechanism driving this preferential grazing is unclear, Evans and Wilson (2008) proposed possible changes in prey size, motility, nutritional value, palatability, and chemical cues as potential causes.

However, to the best of our knowledge, those results have not yet been reproduced in any independent studies. Also, one aspect that was not investigated is *if* and *how* preferential grazing on infected *E. huxleyi* might modify the transfer of C and essential nutrients up the food web. In this study we investigated the effect of viral infection on the growth and ingestion rates, cell volume, and FA composition of *O. marina* cells to better understand how the grazing behavior and physiology of microzooplankton is influenced by viral infection of abundant and important phytoplankton prey.

MATERIALS AND METHODS

Culture maintenance:

Clonal *Emiliania huxleyi* strain CCMP 374 (non-axenic, non-calcifying; 3-5µm) and non-axenic clonal *O. marina* strain CCMP 1795 were obtained from the Provasoli-Guillard National Center for Marine Algae and Microbiota (NCMA-Bigelow Laboratory, Maine, USA). A non-axenic clonal *Dunaliella* sp. strain was sourced from the University of South Carolina. *E. huxleyi*, *O. marina,* and *Dunaliella* cultures were maintained at 16 °C under a light:dark cycle (14:10 h; 250 µmoL photons m^{-2} s^{-1}). *E. huxleyi* and *Dunaliella* sp. cultures were kept in exponential growth phase by periodically transferring 10% (v/v) culture into fresh f/2-Si seawater medium (Guillard 1975). *O. marina* stock cultures were fed weekly with fresh *Dunaliella* sp. cultures (5% (v/v)). Fresh EhV-86 (Wilson et al. 2002) lysates were obtained by inoculating *E. huxleyi* cultures in exponential growth phase. Once culture clearance was observed (typically 3 – 5 days post inoculation (p.i.)), cell debris was removed by filtration (0.45 µm PES filter) and the EhV-86 lysates were then stored at 4°C in the dark for up to two weeks prior to being used in an experiment. The same EhV-86 lysate stock was used to determine infection dynamics and for grazing experiments 1 – 3 (see experimental details in the sections

below). Cell and virus concentrations were measured using a FACScan flow cytometer (Beckton Dickinson, Franklin Lakes, NJ), equipped with an air-cooled laser providing 50 mW at 488 nm with standard filter set-up, as previously described (Brussaard 2004; Marie et al. 1999).

Emiliania huxleyi virus infection dynamics:

Fifty milliliter aliquots of exponentially growing *E. huxleyi* culture were inoculated at four EhV-86 to host ratios of 5:1, 20:1, 50:1, and 100:1, in triplicate. Fresh f/2-Si media was added to each flask in order to achieve the same *E. huxleyi* cell concentration in all flasks. Aliquots were taken from each culture at 2, 4, 6, and 20 h p.i. for cell enumeration using flow cytometry (FCM). Cells were stained with the orange fluorescent lipid-specific dye N-(3-Triethylammoniumpropyl)-4-[4-(dibutylamino)styryl] pyridinium dibromide (FM 1-43, Invitrogen Co., Carlsbad, CA, USA) to allow discrimination between visibly infected and non-infected *E. huxleyi* cells (Martínez Martínez et al. 2011) (Fig. S1). Progression of the viral infection was quantified by tracking the percentage of visibly infected *E. huxleyi* over time.

Emiliania huxleyi C and N content:

A culture of *E. huxleyi* at exponential growth phase was divided in two equal volumes. One of the aliquots received EhV-86 to achieve a 50:1 virus:host ratio; the second one received an equal volume of fresh f/2-Si medium to achieve similar cell concentration in both cultures. *Emiliania huxleyi* concentration and percentage of visibly infected cells in each flask was determined immediately after the addition of EhV-86 and f/2-Si medium at 5 h and at 24 h p.i. Six 5 ml samples were taken from each flask immediately after the addition of EhV-86 and f/2-Si medium and at 24 h p.i. and were gravity filtered through a combusted glass fiber filter (Whatman GF/F; GE Healthcare Life Sciences, Pittsburg, PA) to collect particulate matter. The filtrates were then passed through fresh combusted GF/F filters to serve as C and N background

controls (residual dissolved C and N retained by the filters). Filters were stored at -80° C until analysis. Prior to testing, the filters were dried at 45 °C for 24 h before being placed in 9 × 10 mm Costech tin capsules using clean forceps and sample preparation block. Calibration standards were prepared from acetanilide. The samples, standards, and filter blanks were analyzed using a Costech ECS 4010 elemental analyzer (980°C combustion).

Oxyrrhis marina specific growth and grazing rates:

Four independent experiments (experiments 1 – 4) were performed. *Oxyrrhis marina* was not fed for 3 days prior to each experiment to ensure their feeding vacuoles were empty. FCM was employed to check for the absence of prey-derived chlorophyll red autofluorescence signal within *O. marina* vacuoles after the 3-day period. Stock *E. huxleyi* cultures (~1×10^6 cells ml^{-1}) were split into two equal volumes. One of the flasks was inoculated with fresh EhV-86 lysates to achieve the virus:host ratios specified for each experiment in Table 1. The second flask received f/2-Si media equal to the virus stock volume to match the dilution of cells. The flasks were incubated without shaking under the standard culture conditions indicated above. Incubations were carried out for 6 h to allow sufficient viral infection levels (see results from virus infection dynamics below, Fig.1). Equal volume aliquots of either infected or non-infected *E. huxleyi* cultures were fed to triplicate *O. marina* cultures. Additional aliquots of the *E. huxleyi* cultures (infected and non-infected) were maintained separately as non-grazing controls. It should be noted that non-grazing control cultures were not maintained during experiment 3, instead, average *E. huxleyi* growth rates from experiment 2 were used to normalize for *E. huxleyi* cell growth and lysis. Both these experiments employed the same EhV stock, virus:host ratio, and culture volume, and only differed in the length of time of the experiment (Table 1). We have shown in this study and elsewhere (Gilg et al. 2016; Vermont et al. 2016) that under comparable

conditions infection dynamics and virus production are highly reproducible. *E. huxleyi* and *O. marina* cell concentrations were monitored in each flask by FCM. Prey and predator cell concentrations were measured immediately after the initial feeding and every 30 min for the first 2 h and then every hour up to 6 h for experiment 1 (Fig. S2) and every 24 h for experiments 2 – 4. During experiments 2 – 4 *O. marina* cultures were fed, either infected (6 h after virus addition) or non-infected *E. huxleyi* cultures, immediately after determining cell concentrations at the end of each 24 h incubation period for a total of 3 – 7 days (Table 1). The time length of our experiments is ecologically relevant and representative of high rates of viral infection during induced blooms of mixed assemblies of *E. huxleyi* (Castberg et al. 2001; Martínez Martínez et al. 2007). Fresh prey cell additions were calculated to bring the prey:predator ratio to the same level as at the beginning of the experiment. Sterile f/2-Si medium was added, as needed, to the *O. marina* cultures to maintain comparable cell concentration between treatments. Additional experimental design information can be found in Table 1. *Oxyrrhis marina* specific growth and grazing rates were determined by the equations of Frost (1972) and used to calculate *O. marina* growth per *E. huxleyi* cell consumed.

Projected Oxyrrhis marina's abundance:

The removal of cells within samples collected at each time point together with the subsequent additions of fresh prey cells and f/2-Si medium to maintain prey and predator cell concentrations at near to initial concentrations hindered direct measurement of total *O. marina* production and prey cells consumed. Consequently, we performed a mathematical projection to estimate both consumption and production of *O. marina*. Average growth and grazing rates of individual cultures from experiments 2 – 4 (n=9) were combined to calculate the overall average ± 1 standard error (SE) growth and grazing rates of *O. marina* fed either infected or non-infected

E. huxleyi cells. We postulated a starting population size of 6,000 *O. marina* cells and assumed *E. huxleyi* prey saturation and no mortality for *O. marina* over a 7-day period. We applied the overall *O. marina*'s average ± 1 SE growth rate over the 7-day period to calculate a reasonable abundance range for each diet. We then used the equations of Frost (1972) with the overall *O. marina*'s average ± 1 SE grazing rates and the hypothetical population size calculated above to predict the potential total ingestion of *E. huxleyi* cells under such scenario.

Oxyrrhis marina and E. huxleyi fatty acid (FA) analysis:

The effect of feeding on virally infected or non-infected *E. huxleyi* on the FA composition of *O. marina* was investigated during experiment 2. Aliquots of 5 ml for FA analysis were taken from non-infected *E. huxleyi* cultures and from cultures 6 h after inoculation with EhV-86 (in duplicate), as well as from *O. marina* cultures (in triplicate) before feeding them with *E. huxleyi* cells (Day 0) and after three days being fed *E. huxleyi* (Day 3). Samples were vacuum filtered through a combusted glass fiber filter (Whatman GF/F; GE Healthcare Life Sciences, Pittsburg, PA), and stored at -80° C until analysis. FAs were converted to FA methyl esters (FAMEs) in a one-step extraction direct methanolysis process (Meier et al. 2006) following the procedures detailed in Jacobsen et al. (2012). FAMEs were analyzed on a gas chromatograph with mass spectrometric detector (Shimadzu GCMS-QP2010 Ultra, Shimadzu Scientific Instruments, Columbia, MD). FAME samples were reconstituted in 200 µl of hexane and 1 µl was injected into the GC/MS injector which was kept at 250°C. FAMEs were separated on a SGE BPX-70 column, in a helium mobile phase at a flow rate of 1.17 ml min^{-1}. A Supelco 37 Component FAME Mix (47885-U; Supelco Analytical, Bellefonte, PA) standard solution was used for instrument calibration. Individual FAMEs were identified via comparison to standard mixture peak retention times and fragmentation patterns using the NIST-library of compound

mass spectra. FAME concentrations were calculated from peak area relative to that of a C19:0 internal standard that was added to each sample prior to extraction. FA type concentrations were converted to percentages of the combined total FA concentration.

Oxyrrhis marina cell volume:

Aliquots of 500 µl were taken from a prey-depleted *O. marina* culture (i.e., 3 days without being fed *Dunaliella* sp. cells or any other prey type) and once a day for three days from each *O. marina* culture during experiment 4. Fixation is required to immobilize the dinoflagellate cells to facilitate light microscopy examination. Common fixatives such as Lugol's or glutaraldehyde alter cell volume (Menden-Deuer et al. 2001). Alternatively, live cells can be immobilized by adding nickel sulfate (0.003% final concentration), which appears to have no effect on cell shape and size (Menden-Deuer et al. 2001). We chose to fix culture *O. marina* culture aliquots by transferring 50% (v/v) into 70% ethanol and storing at 4°C for 30 minutes prior to analysis. Ethanol did not appear to alter cell size since our results were very similar to the measurements with added nickel sulfate from Menden-Deuer et al. (2001); however, no direct comparison of these two methods was carried out. Ten randomly selected individual *O. marina* cells from each aliquot were photographed on a hemocytometer. The hemocytometer gridding served as scale for cell sizing. Images were and measured for cell width and length using ImageJ (Schneider et al. 2012). Volume was calculated for each cell using the equation for the volume of a rotational ellipsoid; $V=\frac{\pi}{6}\ x\ d^2 x\ h$ (Edler 1979; Menden-Deuer & Lessard 2000). In this calculation we assume that the width and depth of *O. marina* were equal. Differences in cell volume between treatments were evaluated using a standard t-test. Total C per *O. marina* cell was estimated based on the average cell volume using the equation log pg C $cell^{-1}$ = -0.665 + log vol × 0.939 (Menden-Deuer & Lessard 2000).

Statistical analyses:

Temporal differences within the same diet treatment for *E. huxleyi* C and N content and for *O. marina* specific growth and ingestion rates, and cell volume were analyzed with a two-tailed, paired t-test, Alpha level 0.01. When comparing parameters between treatments and for FA composition, the differences were analyzed with a two-tailed, unpaired t-test assuming equal variance, Alpha level 0.01. P-values (P) < 0.05 were significant and $P < 0.01$ were considered highly significant.

RESULTS

Emiliania huxleyi virus infection dynamics:

The percentage of visibly infected cells (as revealed by FCM) increased at higher virus:host inoculation ratios over a 20 h period. During this same period cell abundance did not change significantly in virally-infected cultures compared to non-infected cultures (Fig. S1C). The highest virus:host ratio (100:1) yielded ~19% visibly infected *E. huxleyi* cells by 6 h p.i., and ~57% by 20 h p.i. (Fig. 1); consequently we chose this ratio for experiments 1 – 3, which were carried out with the same EhV-86 stock and under the same environmental conditions employed to determine the infection dynamics (Fig. 1). The infection dynamics of *E. huxleyi* (CCMP374) and viral (EhV-86) production are highly consistent and reproducible when using the same host and virus strains and conditions, in particular when using the same virus lysate stock for a series of experiments within 2-4 weeks (Gilg et al. 2016; Vermont et al. 2016). Infected cells begin to release virus progeny at around 4.5 h p.i. (Mackinder et al. 2009) and any cells not infected by the initial EhV inoculum can become infected during successive infection rounds by the new EhV progeny. At the high virus:host ratios in our study, close to 100% of the *E. huxleyi* cells become infected by 24 h p.i. (Gilg et al. 2016; Vermont et al. 2016), even if not evident by FCM

(Martínez Martínez et al. 2011). In experiment 4, in which we used a fresh EhV-86 lysate stock and carried out the inoculations at a 50:1 virus:host ratio, 36% of *E. huxleyi* cells were visibly infected by 6 h p.i.

Emiliania huxleyi C and N content:

Over a 24h incubation, both infected and non-infected cultures of *E. huxleyi* exhibited a slight but significant increase ($P = 4.94 \times 10^{-4}$ and $P = 0.018$, respectively) in C content of 9.27 ± 0.19 to 10.86 ± 0.43 pg C cell^{-1} (± SD) for infected cells and 8.94 ± 0.94 to 10.42 ± 0.26 pg C cell^{-1} for non-infected cells, respectively. Carbon content was not statistically different between treatments ($P = 0.42$ at t0 and $P = 0.057$ at t24) (Fig. 2A, Table S1). *Emiliania huxleyi* N content was not statistically different between samples at the beginning of the experiment ($P = 0.989$), but it increased significantly over the 24 h incubation; from 1.51 ± 0.08 to 1.89 ± 0.13 pg N cell^{-1} (± SD) ($P = 6.36 \times 10^{-4}$) for infected cells and 1.51 ± 0.05 to 2.09 ± 0.07 pg N cell^{-1} ($P = 1.80 \times 10^{-5}$) for non-infected cells, respectively. The N content of non-infected cells was significantly higher than in non-infected cells after the 24 h incubations ($P = 0.008$) (Fig. 2B).

Oxyrrhis marina specific growth rate:

The 6 h duration of experiment 1 was too short to measure *O. marina* growth rates. In the longer experiments, the growth rates (experiments 2-4) of *O. marina* ranged from 0.28 to 0.43 day^{-1} (average 0.35 ± 0.08 day^{-1} (± SD)) when fed non-infected prey and from 0.47 to 0.56 day^{-1} (average 0.52 ± 0.05 day^{-1}) when fed infected prey (Fig. 3A, Table S2). Specifically, *O. marina* specific growth rates were 30% ($P = 0.002$), 43.4% ($P = 5.29 \times 10^{-6}$), and 91.3% ($P = 0.006$) higher when fed infected *E. huxleyi* during experiments 2, 3, and 4, respectively (Fig. 3 A). Based on the average growth rates, and assuming no loss term for *O. marina* cells, we calculated

an increase of *O. marina* cells over a 7-day period that is 233% higher with a diet of infected than with a diet of non-infected *E. huxleyi* cells (Fig. 3D).

Oxyrrhis marina ingestion rates:

During the initial 1.9 h in experiment 1, *O. marina* ingestions rates were not significantly different ($P = 0.68$) when feeding on infected (14.48 ± 0.18 cells Om^{-1} h^{-1} (± SD)) vs uninfected cells (14.88 ± 1.57 cells h^{-1}). Between 1.9 and 6 h no additional ingestion was measurable (Fig. 3B, Fig. S2, Table S2). Initial pulse-feeding following a period of starvation is commonly observed in grazing experiments and it is likely the reason for the equal ingestion rates we measured in experiment 1. The combined results from grazing experiments 2 – 4 yielded ingestion rates that were on average 35.4% lower ($P = 0.001$) for *O. marina* fed infected (39.74 ± 12.14 cells Om^{-1} day^{-1}) versus non-infected *E. huxleyi* cells (60.34 ± 10.13 cells Om^{-1} day^{-1}) (Fig. 3B, Table S3). Compared to experiment 1, the higher total number of ingested *E. huxleyi* cells, both infected and non-infected, measured in experiments 2 – 4 indicated that *O. marina* resumed ingestion after 6 h, as prey cells were digested. Also, the relatively low standard deviation values indicated daily ingestion rates were fairly constant from day to day in experiments 2 – 4. Normalizing *O. marina* growth rate to the number of cells ingested renders the highly significant ($P = 1.60 \times 10^{-5}$) differences between diets even more striking (i.e., 86.30%, 238.62%, and 154.44% higher when fed infected *E. huxleyi* cells, for experiments 2, 3, and 4 respectively) (Fig. 3C, Table S2).Combining the higher growth rate of *O. marina* (i.e., higher end abundance, Fig. 3D) and the average ingestion rates (Fig. 3B), we estimated that the total consumption of virus-infected *E. huxleyi* cells would exceed that of non-infected cells after 4 – 5 days and would be on average 63.2% higher for virus-infected *E. huxleyi* over a 7-day period (Fig. 3E).

Oxyrrhis marina and E. huxleyi fatty acid analysis:

Minor differences were detected in the proportions of individual FAs between non-infected and recently-infected *E. huxleyi* cultures (Table 2). Similarly, minor differences in the FA profile were observed in *O. marina* that had consumed infected versus non-infected cells. The cultures containing *O. marina* fed infected *E. huxleyi* contained slightly higher proportions of C17:0 and 2-fold higher proportions of C20:2 (Table 2).

Oxyrrhis marina cell volume:

The average volume of *O. marina* cells was not significantly different ($P = 0.21$) between individuals fed a diet of infected (5226 ± 1267 μm^3 (± SD)) versus non-infected (4706 ± 1259 μm^3) *E. huxleyi* cells (Table 3, Fig. S3).

DISCUSSION

The results presented here show compelling evidence that feeding on virus-infected *E. huxleyi* fuels *O. marina* specific growth, but it does not significantly alter their FA profile and cell size. Furthermore, we show that the higher growth rates of *O. marina* were not due to higher ingestion rates of infected cells or to a tradeoff of *O. marina* cells becoming smaller (i.e., containing less C and nutrients per cell). Consequently, the higher growth efficiencies of *O. marina* feeding on virally infected *E. huxleyi* cells suggest that viral infection of prey cells increases the production of microzooplankton. These results suggest a shift in the "viral shunt" paradigm by pointing toward the flow of organic matter to higher trophic levels being enhanced by viral infection of algae rather than just being short-circuited.

Oxyrrhris marina feed and grow on a wide range of prey types, some prey enhance growth rates more than others (Montagnes et al. 2011). Indeed this study shows that virus-infected *E. huxleyi* cells supported higher *O. marina* growth than non-infected *E. huxleyi* cells, despite lower ingestion rates, suggesting higher nutritional value or higher assimilation

efficiency of infected prey cells. It is worth noting that *O. marina* ingestion rates on virally infected *E. huxleyi* cultures might have been overestimated. A reduction in prey abundance due to viral lysis over each 24 h interval, prior to fresh-prey replenishment, during the experiments might have led to temporarily reduced grazer-prey encounter and ingestion rates. Under such scenario *O. marina*'s growth per ingested infected cell would have be even larger than we estimated, adding further significance to our results. Consequently, our study would represent a conservative estimate of C transfer efficiency.

Based on our measurements, the mechanisms underlying the lower ingestion rates and higher growth efficiency remain unknown. Calcification reduces digestion efficiency and predator growth (Harvey et al. 2015). In the environment, *E. huxleyi* cells lose their liths during an active viral infection (Brussaard et al. 1996; Frada et al. 2008; Jacquet et al. 2002). In this study we chose a non-calcifying *E. huxleyi* strain to uncouple the effects of calcification and prey size, on feeding and growth rates. Furthermore, we found no differences between C content in infected and non-infected *E. huxleyi* cells, while N content was only slightly higher in non-infected cells. Nitrogen depletion in some prey cells causes *O. marina* to cease grazing, possibly due to the buildup of an inhibitor or a change in prey recognition (Flynn et al. 1996; Martel 2009). However, C:N ratios in all of our *E. huxleyi* cultures (virus-infected or not) were lower than 6.6, indicative that N was replete (Davidson et al. 2005; Flynn et al. 1994). Large dsDNA viruses of eukaryotic algae, such as EhVs, have a high demand of C, N and P for the production of lipids, proteins, and nucleotides to support typical high burst sizes. Viral infection can modulate host metabolic pathways and nutrient uptake to fulfill the metabolic requirements of viral production (Malitsky et al. 2016; Monier et al. 2017; Monier et al. 2012; Rosenwasser et al. 2014; Wilson et al. 1996). The production of intermediary biomolecules and changes in *E.*

337 *huxleyi*'s lipidome induced by infection with EhV-86 (Evans et al. 2007; Evans et al. 2006;
338 Evans et al. 2009; Malitsky et al. 2016; Rosenwasser et al. 2014; Suzuki & Suzuki 2006) could
339 potentially lead to increasing the nutritional value of infected cells. During EhV infection,
340 changes in biosynthesis pathways result in the production of more highly saturated FAs (Evans et
341 al. 2009; Floge 2014; Malitsky et al. 2016) and the enhanced production of sphingolipids
342 (Pagarete et al. 2009; Rosenwasser et al. 2014). It should be noted that the majority of these
343 virus-induced alterations in lipid composition have been detected after prolonged infection (> 24
344 h) of *E. huxleyi* cultures. At the relatively coarse level of detail in lipid profile carried out in the
345 present study, only minor differences in FA composition were observed between non-infected *E.*
346 *huxleyi* cultures and cultures that had been infected for 6 h (Table 2). This suggests that
347 differences in FA composition between recently-infected and non-infected *E. huxleyi*, were not
348 responsible for the differences in growth rates of *O. marina*. However, it is possible that the
349 relatively small sample volume collected for FA analysis of *E. huxleyi* cells limited the
350 resolution and detection of differences in FA between infected and non-infected *E. huxleyi* cells
351 (Evans et al. 2009; Floge 2014; Malitsky et al. 2016). Alterations in lipid profile between
352 infected and non-infected cells that were not apparent in our analysis, may contribute to the
353 higher growth efficiencies of *O. marina* fed virally infected prey cells. An additional factor that
354 may influence the nutritional value of the phytoplankton prey is P. In addition to providing a
355 much needed resource for viral replication, P-rich phytoplankton cells increase grazing
356 efficiency and secondary production in cladocerans (Elser et al. 2001; Sterner 1993; Urabe &
357 Sterner 1996; Urabe & Watanabe 1992). Low P availability reduces viral replication in *E.*
358 *huxleyi* (Bratbak et al. 1993) and other eukaryotic algae (Maat et al. 2016; Wilson et al. 1996),
359 possibly by limiting the production of nucleic acids. It has been hypothesized that virally

encoded putative phosphate transporters increase accumulation of P in host cells (Monier et al. 2012; Wilson et al. 1996). While to the best of our knowledge this has not been tested during the infection of *E. huxleyi* cells, most available EhV isolates, including EhV-86, carry an *E. huxleyi*-homolog putative phosphate repressible phosphate permease (PPRPP) gene (Martínez Martínez 2006; Nissimov et al. 2011; Nissimov et al. 2012; Wilson et al. 2005), which we hypothesize led to higher P uptake in virally infected cells in our experiments. Additionally, the stoichiometric "light:nutrient hypothesis" poses that low supply of light relative to P yields more P-rich producers (i.e., low tissue C:P ratios) (Sterner et al. 1997); possibly due to the algae allocating high levels of P to light-harvesting cellular machinery and storing excess P intracellularly (Hessen et al. 2002). In our study, *E. huxleyi* cells were grown in P-rich f/2-Si culture medium and both EhV-infected and non-infected cultures were kept under the same light conditions. In addition to the role of the PPRPP gene in P uptake, we hypothesize that virus-induced reduction in *E. huxleyi*'s photochemical efficiency from the early stages of EhV infection (Gilg et al. 2016) might also induce an increased P uptake and intracellular accumulation. While a reduction in photochemical efficiency might translate into lower C fixation rates, our results show that C content was not affected in infected compared to non-infected cells. Phosphorus content in infected and non-infected *E. huxleyi* cells and its impact on grazing warrants investigation in future studies.

E. huxleyi is an important food source at the base of the food chain and grazing pressure influences population and bloom dynamics (Fileman et al. 2002; Olson & Strom 2002). Virus-induced mortality also plays a prominent role in bloom demise (Bratbak et al. 1993; Brussaard et al. 1996; Castberg et al. 2001; Lehahn et al. 2014; Martínez Martínez et al. 2007) and diverts organic C away from upper trophic levels to the dissolved phase, which fuels the microbial

383 loop—"viral shunt" (Wilhelm & Suttle 1999). Our results suggest that viral infection also boosts
384 microzooplankton production. High rates of viral infection can last from a few days (as in this
385 study) to a few weeks during a natural *E. huxleyi* bloom progression (Brussaard et al. 1996;
386 Castberg et al. 2001; Martínez Martínez et al. 2007), which could result in large differences in C
387 flow through the food web. Extrapolating the results in our study, the enhanced growth rates of
388 microzooplankton populations that feed on virally infected phytoplankton cells would lead to
389 more organic C available for higher trophic levels. Thus, contrary to the idea that viral infection
390 leads only to the production of dissolved organic matter (Wilhelm & Suttle 1999), viral
391 infections at the base of the food chain may augment the flow of C to higher trophic levels as
392 well as toward the microbial loop. Although, to the best of our knowledge, the specific functional
393 response of copepods ingestion of *O. marina* fed infected and non-infected *E. huxleyi* has yet to
394 be investigated, nutrition and reproduction rates are enhanced in copepods fed *O. marina* (grown
395 on other phytoplankton diets) compared to copepods that feed directly on small phytoplankton
396 cells (Broglio et al. 2003; Chu et al. 2008; Parrish et al. 2012; Veloza et al. 2006). Phytoplankton
397 are considered the primary producers of long chain n-3 (LCn-3) PUFAs; however, heterotrophic
398 protists such as *O. marina* are also able to produce sterols and essential FAs (e.g., EPA (C20:5 n-
399 3) and DHA (C22:6 n-3)) from lipid precursors (Chu et al. 2008; Klein Breteler et al. 1999; Lund
400 et al. 2008; Veloza et al. 2006), which emphasizes the important role of microzooplankton in
401 trophic upgrading and C transfer and highlights the need for a better quantitative understanding
402 of the factors that influence microzooplankton grazing behavior and secondary production rates.
403 Incorporating quantitative data for viral lysis and the effect of viral infection in grazing behavior
404 and transfer efficiency into ecosystem models is essential for accurate budgeting of C flow
405 throughout the food web in the global marine ecosystem. As a cautionary reminder, when

406 interpreting these results it is important to note that *O. marina* is not typically found in open
407 waters (Yang et al. 2011) and is not likely to be a common natural predator of *E. huxleyi* cells.
408 However *O. marina* is frequently used as a model predator in laboratory-based experiments
409 because of its morphological similarity to a wide variety of heterotrophic and mixotrophic
410 dinoflagellates and its plasticity in feeding behavior allow it to represent a broad range of marine
411 dominant microzooplankton (Lowe et al. 2011; Roberts et al. 2011). Furthermore, several studies
412 have shown that *O. marina* responds in a similar way to other microzooplankton taxa to various
413 experimental stimuli (Strom et al. 2003a; Strom et al. 2003b; Tillmann 2004). *E. huxleyi*'s true
414 protozoan predators in nature have yet to be precisely identified (Wolfe 2000).

415 A final consideration is that the lower ingestion rates of *O. marina* on *E. huxleyi (*strain
416 CCMP374) cells infected with coccolithovirus EhV-86, compared to non-infected cells, are in
417 contrast with an earlier study that used the same virus strain but a different *E. huxleyi* strain
418 (CCMP 1516—non-calcifying) (Evans & Wilson 2008). Strain-specific differences in the
419 ingestion and clearance rates of *O. marina* feeding on *E. huxleyi* (Harvey et al. 2015) might have
420 played a role in our findings. However, in light of our findings, the results from Evans and
421 Wilson (2008) need to be revisited and revalidated and future studies should include multiple
422 strains within a species (predator, prey, and/or virus) to test differences driven by intraspecific
423 diversity. Importantly, future research is needed that focuses on a range of abundant and
424 ecologically meaningful predator-prey-virus systems.

425 CONCLUSIONS

426 Viruses cause biochemical alterations to their *E. huxleyi* host cells to facilitate viral assembly
427 (Gilg et al. 2016; Malitsky et al. 2016; Rosenwasser et al. 2014; Suzuki & Suzuki 2006). The
428 data presented in this study show that changes due to viral infection of *E. huxleyi* cause higher

growth efficiency and an increase in heterotrophic protist production. Despite the faster growth rates, we found no major difference in cell size, total FA content or FA profile of *O. marina* maintained on a diet of virally infected *E. huxleyi* cells during 3 days as compared with *O. marina* individuals reared on non-infected cells for the same period of time. These results suggest that after a feeding period of time of 3 days the nutritional value of *O. marina* is unaffected by the infection status of their *E. huxelyi* diet despite known changes in the FA profiles and biochemical pathways in EhV-86 infected *E. huxleyi* cells. Combined, these results suggest that during viral infection of *E. huxleyi,* there may be a proportionally increased flow of C to higher trophic levels. Thus, in addition to the “viral shunt" hypothesis, these results suggest that food webs with virally infected *E. huxleyi* cells may shunt proportionally more C to higher trophic levels than non-infected systems. In order to gain a more comprehensive understanding of ocean ecosystem function in relation to C flow, it is crucial that we get quantitative knowledge of each of those processes and the factors that determine the relative magnitude of each pathway. The significance of our work is that, given the global scale and rapid dynamics of viral infections in the ocean, infection of primary producers is likely to be one of the compounding factors that influences the qualitative and quantitative flow of C in oceanic systems and determines overall efficiency of transfer to higher trophic levels.

ACKNOWLEDGEMENTS

We acknowledge Bigelow Analytical Services for the analysis of the fatty acid and particulate carbon and nitrogen content.

FUNDING

This research was supported by funds from the National Science Foundation through Grant EAR 1460861 – REU Site: Bigelow Laboratory for Ocean Sciences – Undergraduate

452 Research Experience in the Gulf of Maine and the World Ocean, , Gordon and Betty Moore
453 Foundation Grant GBMF3397, and by Bigelow Laboratory for Ocean Sciences and the
454 University of Maine internal funding.

455 REFERENCES

456 Bratbak G, Egge JK, and Heldal M. 1993. Viral mortality of the marine alga *Emiliania huxleyi*
457 (Haptophyceae) and termination of algal blooms. *Mar Ecol-Prog Ser* 93:39-48.

458 Broglio E, Jónasdóttir SH, Calbet A, Jakobsen HH, and Saiz E. 2003. Effect of heterotrophic
459 versus autotrophic food on feeding and reproduction of the calanoid copepod Acartia tonsa:
460 relationship with prey fatty acid composition. *Aquatic Microbial Ecology* 31:267-278.

461 Brussaard CPD. 2004. Optimization of procedures for counting viruses by flow cytometry. *Appl*
462 *Environ Microbiol* 70:1506-1513.

463 Brussaard CPD, Kempers RS, Kop AJ, Riegman R, and Heldal M. 1996. Virus-like particles in a
464 summer bloom of *Emiliania huxleyi* in the North Sea. *Aquatic Microbial Ecology* 10:105-
465 113.

466 Castberg T, Larsen A, Sandaa RA, Brussaard CPD, Egge JK, Heldal M, Thyrhaug R, van
467 Hannen EJ, and Bratbak G. 2001. Microbial population dynamics and diversity during a
468 bloom of the marine coccolithophorid *Emiliania huxleyi* (Haptophyta). *Marine Ecology-*
469 *Progress Series* 221:39 - 46.

470 Chu FLE, Lund ED, and Podbesek JA. 2008. Quantitative significance of n-3 essential fatty acid
471 contribution by heterotrophic protists in marine pelagic food webs. *Marine Ecology*
472 *Progress Series* 354:85-95.

473 Davidson K, Roberts EC, Wilson AM, and Mitchell E. 2005. The Role of Prey Nutritional Status
474 in Governing Protozoan Nitrogen Regeneration Efficiency. *Protist* 156:45-62.
475 http://dx.doi.org/10.1016/j.protis.2004.10.001
476 Edler L. 1979. Phytoplankton and chlorophyll: Recommendations on methods for marine
477 biological studies in the Baltic Sea. . *Baltic Marine Biologists Publication* 5:1-38.
478 Elser JJ, Hayakawa K, and Urabe J. 2001. NUTRIENT LIMITATION REDUCES FOOD
479 QUALITY FOR ZOOPLANKTON: DAPHNIA RESPONSE TO SESTON PHOSPHORUS
480 ENRICHMENT. *Ecology* 82:898-903. 10.1890/0012-
481 9658(2001)082[0898:NLRFQF]2.0.CO;2
482 Evans C, Kadner SV, Darroch LJ, Wilson WH, Liss PS, and Malin G. 2007. The Relative
483 Significance of Viral Lysis and Microzooplankton Grazing as Pathways of
484 Dimethylsulfoniopropionate (DMSP) Cleavage: An Emiliania huxleyi Culture Study.
485 *Limnology and Oceanography* 52:1036-1045.
486 Evans C, Malin G, Mills GP, and Wilson WH. 2006. Viral infection of *Emiliania huxleyi*
487 (Prymnesiophyceae) leads to elevated production of reactive oxygen species. *J Phycol*
488 42:1040-1047. doi:10.1111/j.1529-8817.2006.00256.x
489 Evans C, Pond DW, and Wilson WH. 2009. Changes in Emiliania huxleyi fatty acid profiles
490 during infection with E. huxleyi virus 86: physiological and ecological implications. *Aquatic*
491 *Microbial Ecology* 55:219-228. 10.3354/ame01295
492 Evans C, and Wilson WH. 2008. Preferential grazing of Oxyrrhis marina on virus infected
493 Emiliania huxleyi. *Limnology and Oceanography* 53:2035-2040. 10.4319/lo.2008.53.5.2035
494 Fileman ES, Cummings DG, and Llewellyn CA. 2002. Microplankton community structure and
495 the impact of microzooplankton grazing during an Emiliania huxleyi bloom, off the Devon

coast. *Journal of the Marine Biological Association of the United Kingdom* 82:359-368. 10.1017/S0025315402005593

Floge S. 2014. Virus infections of eukaryotic viruses PhD. University of Maine.

Flynn KJ, Davidson K, and Cunningham A. 1996. Prey selection and rejection by a microflagellate; implications for the study and operation of microbial food webs. *Journal of Experimental Marine Biology and Ecology* 196:357-372. http://dx.doi.org/10.1016/0022-0981(95)00140-9

Flynn KJ, Davidson K, and Leftley JW. 1994. Carbon-nitrogen relations at whole-cell and free-amino-acid levels during batch growth of Isochrysis galbana (Prymnesiophyceae) under conditions of alternating light and dark. *Marine Biology* 118:229-237. 10.1007/bf00349789

Frada M, Probert I, Allen MJ, Wilson WH, and de Vargas C. 2008. The 'Cheshire Cat' escape strategy of the coccolithophore Emiliania huxleyi in response to viral infection. *P Natl Acad Sci USA* 105:15944-15949. 10.1073/pnas.0807707105

Frost BW. 1972. Effects of size and concentration of food particles on the feeding behavior of the marine planktonic copepod *Calanus pacificus*. *Limnology and Oceanography* 17:805-815. 10.4319/lo.1972.17.6.0805

Gilg IC, Archer SD, Floge SA, Fields DM, Vermont AI, Leavitt AH, Wilson WH, and Martínez Martínez J. 2016. Differential gene expression is tied to photochemical efficiency reduction in virally infected Emiliania huxleyi. *Marine Ecology Progress Series* 555:13-27.

Guillard RRL. 1975. Culture of phytoplankton for feeding marine invertebrates. In: Smith WL, and Chanley MH, eds. *Culture of marine invertebrate animals*. New York: Plenum Press, 29-60.

518 Harvey EL, Bidle KD, and Johnson MD. 2015. Consequences of strain variability and
519 calcification in Emiliania huxleyi on microzooplankton grazing. *Journal of Plankton*
520 *Research* 37:1137-1148. 10.1093/plankt/fbv081
521 Hessen DO, Færøvig PJ, and Andersen T. 2002. Light, nutrients, ans P:C ratios in algae: Grazer
522 performance related to food quality and quantity. *Ecology* 83:1886-1898. 10.1890/0012-
523 9658(2002)083[1886:LNAPCR]2.0.CO;2
524 Holligan PM, Fernandez E, Aiken J, Balch WM, Boyd P, Burkill PH, Finch M, Groom SB,
525 Malin G, Muller K, Purdie DA, Robinson C, Trees CC, Turner SM, and Vanderwal P. 1993.
526 A biogeochemical study of the coccolithophore, *Emiliania huxleyi,* in the North-Atlantic.
527 *Global Biogeochem Cy* 7:879-900.
528 Jacobsen A, Grahl-Nielsen O, and Magnesen T. 2012. Effects of reduced diameter of bag
529 cultures on content of essential fatty acids and cell density in a continuous algal production
530 system. *Journal of Applied Phycology* 24:109-116. 10.1007/s10811-011-9655-6
531 Jacquet S, Heldal M, Iglesias-Rodriguez D, Larsen A, Wilson W, and Bratbak G. 2002. Flow
532 cytometric analysis of an *Emiliana huxleyi* bloom terminated by viral infection. *Aquatic*
533 *Microbial Ecology* 27:111-124.
534 Klein Breteler WCM, Schogt N, Baas M, Schouten S, and Kraay GW. 1999. Trophic upgrading
535 of food quality by protozoans enhancing copepod growth: role of essential lipids. *Marine*
536 *Biology* 135:191-198. 10.1007/s002270050616
537 Lehahn Y, Koren I, Schatz D, Frada M, Sheyn U, Boss E, Efrati S, Rudich Y, Trainic M,
538 Sharoni S, Laber C, DiTullio Giacomo R, Coolen Marco JL, Martins Ana M, Van Mooy
539 Benjamin AS, Bidle Kay D, and Vardi A. 2014. Decoupling Physical from Biological

Processes to Assess the Impact of Viruses on a Mesoscale Algal Bloom. *Current Biology* 24:2041-2046. 10.1016/j.cub.2014.07.046

Lowe CD, Martin LE, Roberts EC, Watts PC, Wootton EC, and Montagnes DJS. 2011. Collection, isolation and culturing strategies for Oxyrrhis marina. *Journal of Plankton Research* 33:569-578. 10.1093/plankt/fbq161

Lund ED, Chu F-LE, Harvey E, and Adlof R. 2008. Mechanism(s) of long chain n-3 essential fatty acid production in two species of heterotrophic protists: Oxyrrhis marina and Gyrodinium dominans. *Marine Biology* 155:23-36. 10.1007/s00227-008-1003-2

Maat DS, and Brussaard CPD. 2016. Both phosphorus- and nitrogen limitation constrain viral proliferation in marine phytoplankton. *Aquatic Microbial Ecology* 77:87-97.

Maat DS, van Bleijswijk JDL, Witte HJ, and Brussaard CPD. 2016. Virus production in phosphorus-limited Micromonas pusilla stimulated by a supply of naturally low concentrations of different phosphorus sources, far into the lytic cycle. *FEMS Microbiology Ecology* 92:fiw136-fiw136. 10.1093/femsec/fiw136

Mackinder LCM, Worthy CA, Biggi G, Hall M, Ryan KP, Varsani A, Harper G, Wilson WH, Brownlee C, and Schroeder DC. 2009. A unicelular algal virus, *Emiliania huxleyi* virus 86, exploits an animal-like infection strategy. *J Gen Virol* 90:2306-2316.

Malitsky S, Ziv C, Rosenwasser S, Zheng S, Schatz D, Porat Z, Ben-Dor S, Aharoni A, and Vardi A. 2016. Viral infection of the marine alga Emiliania huxleyi triggers lipidome remodeling and induces the production of highly saturated triacylglycerol. *New Phytologist* 210:88-96. 10.1111/nph.13852

561 Marie D, Brussaard CPD, Thyrhaug R, Bratbak G, and Vaulot D. 1999. Enumeration of marine
562 viruses in culture and natural samples by flow cytometry. *Applied and Environmental*
563 *Microbiology* 65:45-52.
564 Martel CM. 2009. Conceptual Bases for Prey Biorecognition and Feeding Selectivity in the
565 Microplanktonic Marine Phagotroph Oxyrrhis marina. *Microbial Ecology* 57:589-597.
566 10.1007/s00248-008-9421-8
567 Martínez Martínez J. 2006. Molecular ecology of marine algal viruses Ph.D. University of
568 Plymouth.
569 Martínez Martínez J, Norland S, Thingstad F, Schroeder DC, Bratbak G, Wilson WH, and
570 Larsen A. 2006. Variability in microbial population dynamics between similarly perturbed
571 mesocosms. *Journal of Plankton Research* 28:783-791.
572 Martínez Martínez J, Poulton NJ, Stepanauskas R, Sieracki ME, and Wilson WH. 2011.
573 Targeted Sorting of Single Virus-Infected Cells of the Coccolithophore <italic>Emiliania
574 huxleyi</italic>. *PLoS ONE* 6:e22520.
575 Martínez Martínez J, Schroeder DC, Larsen A, Bratbak G, and Wilson WH. 2007. Molecular
576 dynamics of *Emiliania huxleyi* and cooccurring viruses during two separate mesocosm
577 studies. *Appl Environ Microb* 73:554-562.
578 Meier S, Mjøs SA, Joensen H, and Grahl-Nielsen O. 2006. Validation of a one-step
579 extraction/methylation method for determination of fatty acids and cholesterol in marine
580 tissues. *Journal of Chromatography a* 1104:291-298.
581 http://dx.doi.org/10.1016/j.chroma.2005.11.045

582 Menden-Deuer S, and Lessard EJ. 2000. Carbon to volume relationships for dinoflagellates,
583 diatoms, and other protist plankton. *Limnology and Oceanography* 45:569-579.
584 10.4319/lo.2000.45.3.0569
585 Menden-Deuer S, Lessard EJ, and Satterberg J. 2001. Effect of preservation on dinoflagellate
586 and diatom cell volume and consequences for carbon biomass predictions. *Marine Ecology*
587 *Progress Series* 222:41-50.
588 Mojica KDA, and Brussaard CPD. 2014. Factors affecting virus dynamics and microbial host–
589 virus interactions in marine environments. *FEMS Microbiology Ecology* 89:495-515.
590 10.1111/1574-6941.12343
591 Monier A, Chambouvet A, Milner DS, Attah V, Terrado R, Lovejoy C, Moreau H, Santoro AE,
592 Derelle É, and Richards TA. 2017. Host-derived viral transporter protein for nitrogen uptake
593 in infected marine phytoplankton. *Proceedings of the National Academy of Sciences of the*
594 *United States of America* 114:E7489-E7498. 10.1073/pnas.1708097114
595 Monier A, Welsh RM, Gentemann C, Weinstock G, Sodergren E, Armbrust EV, Eisen JA, and
596 Worden AZ. 2012. Phosphate transporters in marine phytoplankton and their viruses: cross-
597 domain commonalities in viral-host gene exchanges. *Environmental Microbiology* 14:162-
598 176. 10.1111/j.1462-2920.2011.02576.x
599 Montagnes DJS, Lowe CD, Martin L, Watts PC, Downes-Tettmar N, Yang Z, Roberts EC, and
600 Davidson K. 2011. Oxyrrhis marina growth, sex and reproduction. *Journal of Plankton*
601 *Research* 33:615-627. 10.1093/plankt/fbq111
602 Nissimov JI, Worthy CA, Rooks P, Napier JA, Kimmance SA, Henn MR, Ogata H, and Allen
603 MJ. 2011. Draft Genome Sequence of the Coccolithovirus Emiliania huxleyi Virus 203.
604 *Journal of Virology* 85:13468-13469. 10.1128/jvi.06440-11

605 Nissimov JI, Worthy CA, Rooks P, Napier JA, Kimmance SA, Henn MR, Ogata H, and Allen
606 MJ. 2012. Draft Genome Sequence of the Coccolithovirus Emiliania huxleyi Virus 202.
607 *Journal of Virology* 86:2380-2381. 10.1128/jvi.06863-11
608 Olson MB, and Strom SL. 2002. Phytoplankton growth, microzooplankton herbivory and
609 community structure in the southeast Bering Sea: insight into the formation and temporal
610 persistence of an Emiliania huxleyi bloom. *Deep-Sea Research Part Ii-Topical Studies in*
611 *Oceanography* 49:5969-5990.
612 Pagarete A, Allen MJ, Wilson WH, Kimmance SA, and De Vargas C. 2009. Host–virus shift of
613 the sphingolipid pathway along an Emiliania huxleyi bloom: survival of the fattest.
614 *Environmental Microbiology* 11:2840-2848. 10.1111/j.1462-2920.2009.02006.x
615 Parrish CC, French VM, and Whiticar MJ. 2012. Lipid class and fatty acid composition of
616 copepods (Calanus finmarchicus, C. glacialis, Pseudocalanus sp., Tisbe furcata and Nitokra
617 lacustris) fed various combinations of autotrophic and heterotrophic protists. *Journal of*
618 *Plankton Research* 34:356-375. 10.1093/plankt/fbs003
619 Roberts EC, Wootton EC, Davidson K, Jeong HJ, Lowe CD, and Montagnes DJS. 2011. Feeding
620 in the dinoflagellate Oxyrrhis marina: linking behaviour with mechanisms. *Journal of*
621 *Plankton Research* 33:603-614. 10.1093/plankt/fbq118
622 Rosenwasser S, Mausz MA, Schatz D, Sheyn U, Malitsky S, Aharoni A, Weinstock E, Tzfadia
623 O, Ben-Dor S, Feldmesser E, Pohnert G, and Vardi A. 2014. Rewiring Host Lipid
624 Metabolism by Large Viruses Determines the Fate of Emiliania huxleyi, a Bloom-Forming
625 Alga in the Ocean. *The Plant Cell Online* 26:2689-2707. 10.1105/tpc.114.125641
626 Schneider CA, Rasband WS, and Eliceiri KW. 2012. NIH Image to ImageJ: 25 years of image
627 analysis. *Nat Meth* 9:671-675.

628 Sherr EB, and Sherr BF. 2002. Significance of predation by protists in aquatic microbial food
629 webs. *Antonie Van Leeuwenhoek International Journal of General and Molecular*
630 *Microbiology* 81:293-308. 10.1023/a:1020591307260
631 Sherr EB, and Sherr BF. 2009. Capacity of herbivorous protists to control initiation and
632 development of mass phytoplankton blooms. *Aquatic Microbial Ecology* 57:253-262.
633 Sterner RW. 1993. Daphnia Growth on Varying Quality of Scenedesmus: Mineral Limitation of
634 Zooplankton. *Ecology* 74:2351-2360. 10.2307/1939587
635 Sterner RW, Elser JJ, Fee EJ, Guildford SJ, and Chrzanowski TH. 1997. The Light: Nutrient
636 Ratio in Lakes: The Balance of Energy and Materials Affects Ecosystem Structure and
637 Process. *The American Naturalist* 150:663-684. 10.1086/286088
638 Strom S, Wolfe G, Holmes J, Stecher H, Shimeneck C, and Sarah L. 2003a. Chemical defense in
639 the microplankton I: Feeding and growth rates of heterotrophic protists on the DMS-
640 producing phytoplankter Emiliania huxleyi. *Limnology and Oceanography* 48:217-229.
641 10.4319/lo.2003.48.1.0217
642 Strom S, Wolfe G, Slajer A, Lambert S, and Clough J. 2003b. Chemical defense in the
643 microplankton II: Inhibition of protist feeding by β-dimethylsulfoniopropionate (DMSP).
644 *Limnology and Oceanography* 48:230-237. 10.4319/lo.2003.48.1.0230
645 Suttle C. 2005. Viruses in the sea. *Nature* 437:356 - 361.
646 Suttle CA. 1994. The Significance of Viruses to Mortality in Aquatic Microbial Communities.
647 *Microbial Ecology* 28:237-243.
648 Suzuki T, and Suzuki Y. 2006. Virus Infection and Lipid Rafts. *Biological and Pharmaceutical*
649 *Bulletin* 29:1538-1541. 10.1248/bpb.29.1538

650 Thingstad TF. 2000. Elements of a theory for the mechanisms controlling abundance, diversity,
651 and biogeochemical role of lytic bacterial viruses in aquatic systems. *Limnol Oceanogr*
652 45:1320-1328.
653 Tillmann U. 2004. Interactions between Planktonic Microalgae and Protozoan Grazers1. *Journal*
654 *of Eukaryotic Microbiology* 51:156-168. 10.1111/j.1550-7408.2004.tb00540.x
655 Urabe J, and Sterner RW. 1996. Regulation of herbivore growth by the balance of light and
656 nutrients. *Proceedings of the National Academy of Sciences* 93:8465-8469.
657 Urabe J, and Watanabe Y. 1992. Possibility of N or P limitation for planktonic cladocerans: An
658 experimental test. *Limnology and Oceanography* 37:244-251. 10.4319/lo.1992.37.2.0244
659 van Hannen EJ, Zwart G, van Agterveld MP, Gons HJ, Ebert J, and Laanbroek HJ. 1999.
660 Changes in bacterial and eukaryotic community structure after mass lysis of filamentous
661 cyanobacteria associated with viruses. *Applied and Environmental Microbiology* 65:795-
662 801.
663 Veloza AJ, Chu F-LE, and Tang KW. 2006. Trophic modification of essential fatty acids by
664 heterotrophic protists and its effects on the fatty acid composition of the copepod Acartia
665 tonsa. *Marine Biology* 148:779-788. 10.1007/s00227-005-0123-1
666 Vermont A, Martínez Martínez J, Waller J, Gilg I, Leavitt A, Floge S, Archer S, Wilson W, and
667 Fields D. 2016. Virus infection of Emiliania huxleyi deters grazing by the copepod Acartia
668 tonsa. *Journal of Plankton Research* 38:1194-1205. 10.1093/plankt/fbw064
669 Wilhelm SW, and Suttle CA. 1999. Viruses and nutrient cycles in the sea. Viruses play critical
670 roles in the structure and function of aquatic food webs. *Bioscience* 49:781-788.

671 Wilson WH, Carr NG, and Mann NH. 1996. The effect of phosphate status on the kinetics of
672 cyanophage infection in the oceanic cyanobacterium *Synechococcus* sp WH7803. *Journal of*
673 *Phycology* 32:506-516.
674 Wilson WH, Schroeder DC, Allen MJ, Holden M, Parkhill J, Barrell BG, Churcher C, Hamlin N,
675 Mungall K, Norbertczak H, Quail MA, Price CC, Rabbinowitsch E, Walker D, Craigon M,
676 Roy D, and Ghazal P. 2005. Complete genome sequence and lytic phase transcription
677 profile of a *Coccolithovirus*. *Science* 309:1090-1092.
678 Wilson WH, Tarran GA, Schroeder D, Cox M, Oke J, and Malin G. 2002. Isolation of viruses
679 responsible for the demise of an *Emiliania huxleyi* bloom in the English Channel. *J Mar*
680 *Biol Assoc UK* 82:369-377.
681 Yang Z, Jeong HJ, and Montagnes DJS. 2011. The role of Oxyrrhis marina as a model prey:
682 current work and future directions. *Journal of Plankton Research* 33:665-675.
683 10.1093/plankt/fbq112

684
685
686
687
688
689
690
691
692
693

Figure 1

Infection progression of *E. huxleyi*

Fig. 1. Infection progression of *E. huxleyi* at four different virus:host ratios; 5:1, 20:1, 50:1, and 100:1. Values are mean percentage (%) of cells visibly infected over time (hours) ± one standard deviation.

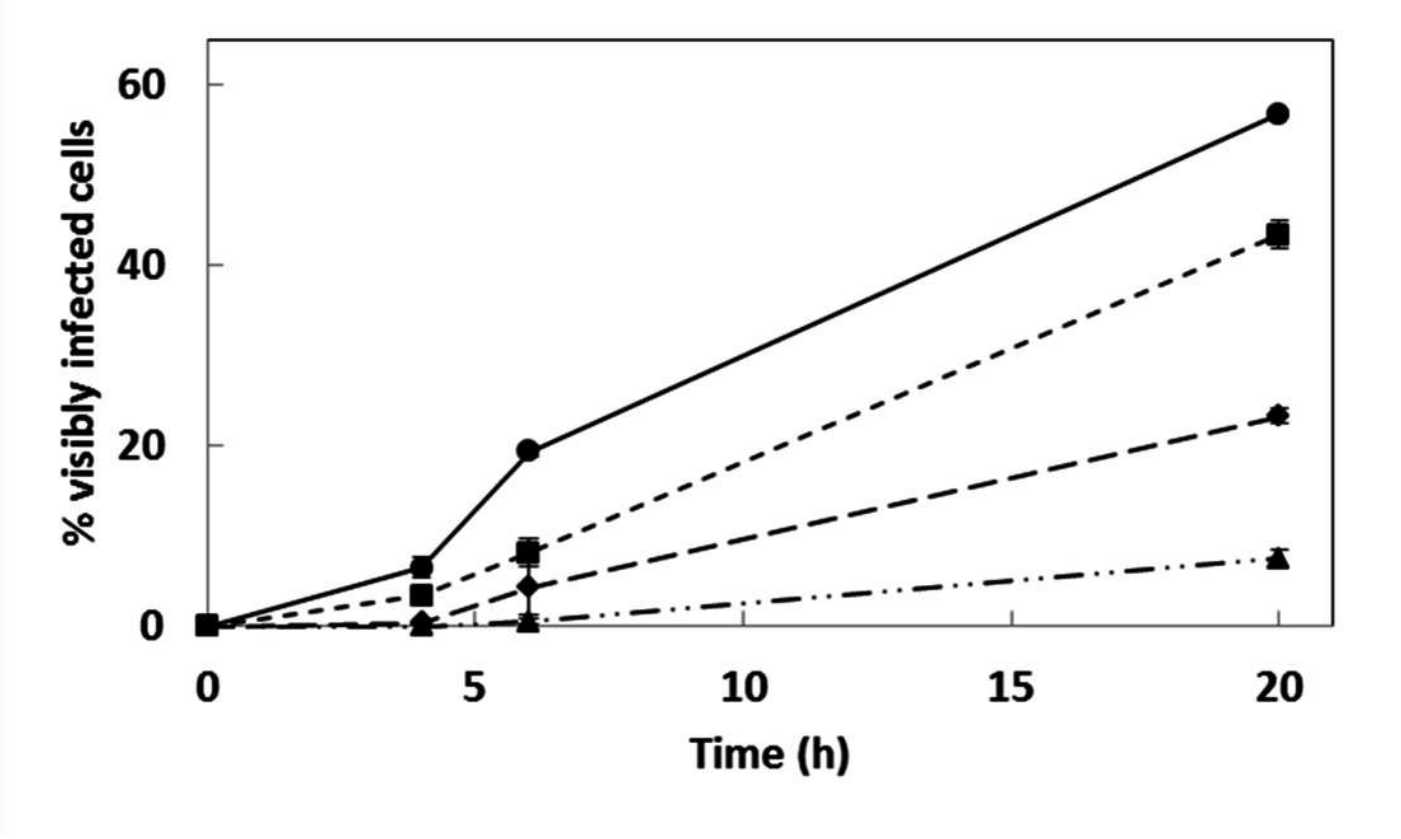

Figure 2

E. huxleyi C and N concentration

Fig. 2. *E. huxleyi* C (**A**) and N (**B**) concentration (pg cell^{-1}) at 0 and 24 hours p.i. Values are mean ± one standard deviation. Letters indicate statistical similarity. Same letters indicate no statistical significance between compared treatments and different letters denote statistical significance.

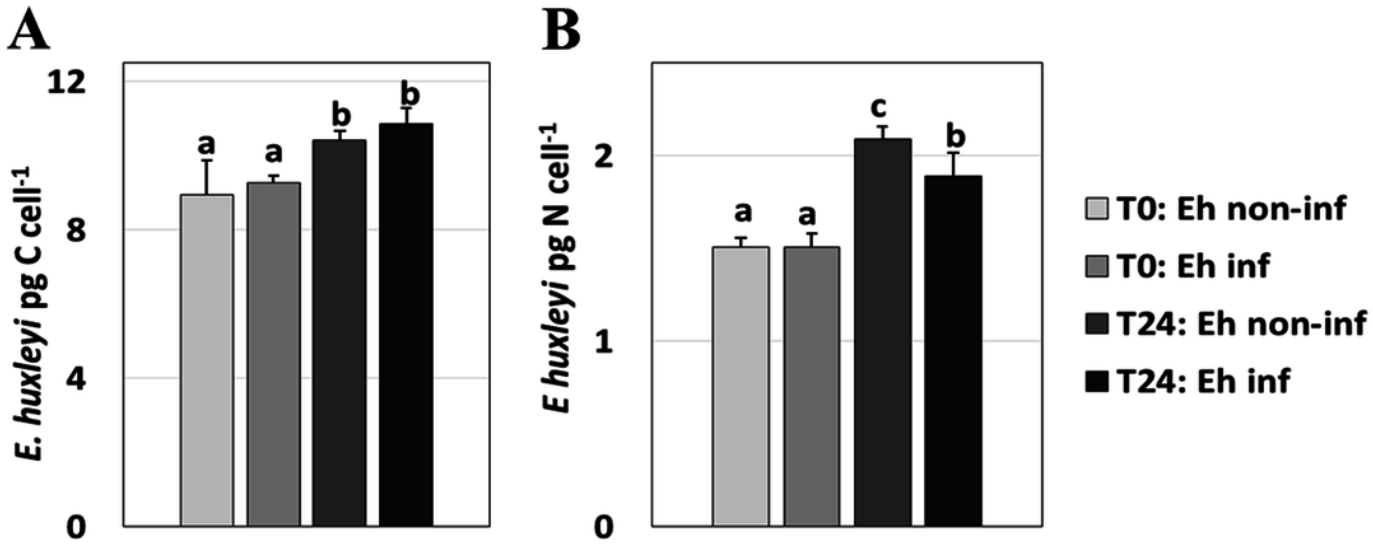

Figure 3

Growth and grazing rates

Fig. 3. Differential growth and grazing rates of *O. marina* fed non-infected versus infected *E. huxleyi*. **A**: *O. marina* growth rates (day $^{-1}$). **B**: *O. marina* grazing rates (Cells Om^{-1} h^{-1} or day^{-1}). **C**: *O. marina* growth rate divided by grazing rate (*O. marina* divided per *E. huxleyi* consumed). Values mean ± one standard deviation (Experiments 2, 3, and 4) and standard deviation (Experiment 1). **D**: Projected abundance of *O. marina*. **E**: Projected total consumption of *E. huxleyi*. Dashed lines are average values and shaded regions are one standard error from Experiments 2, 3, and 4. Asterisks indicate statistical significance: *** $p < 0.001$, ** $p < 0.01$, * $p < 0.05$.

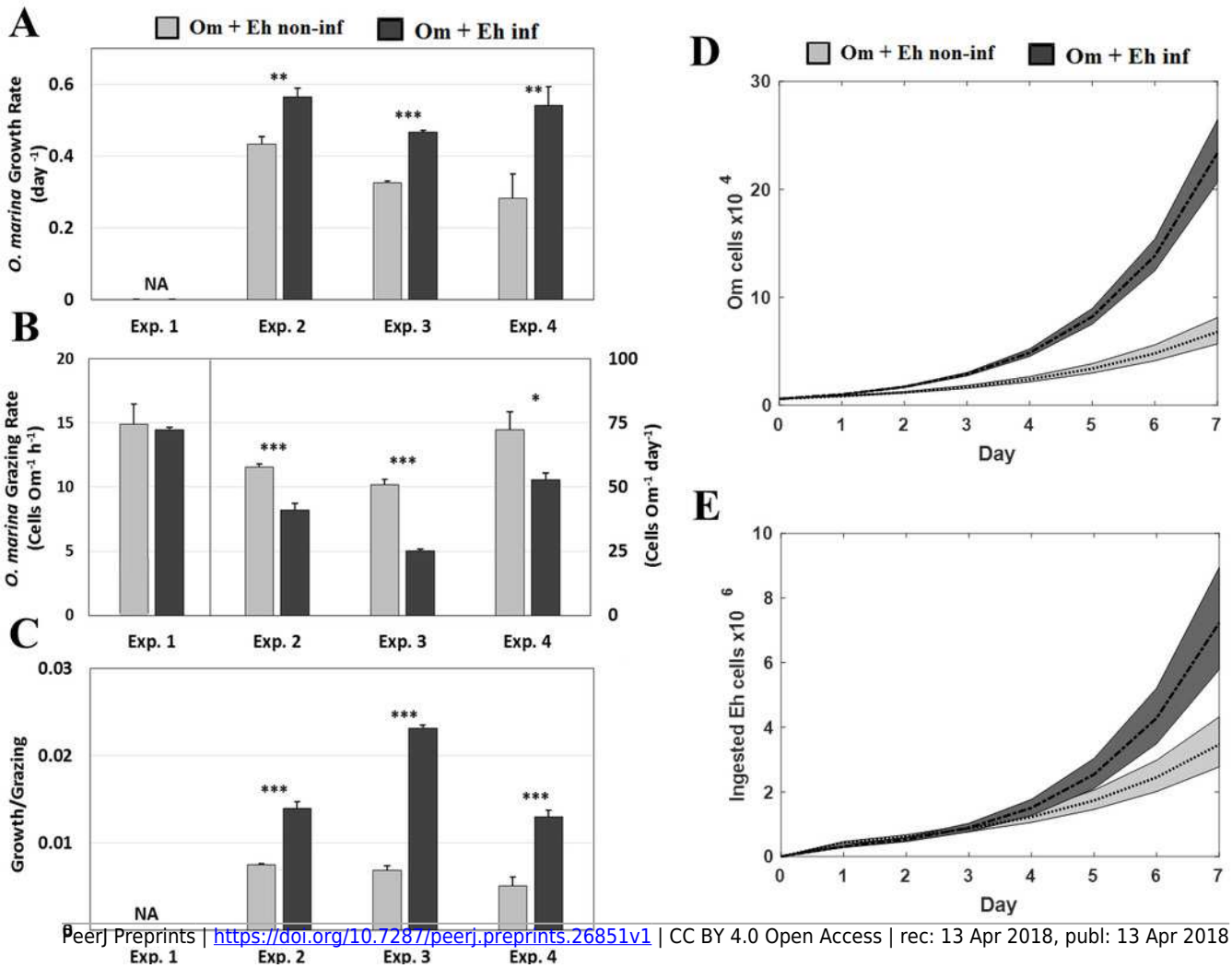

Table 1(on next page)

Table 1. Details of experiments performed.

Emiliania huxleyi (Eh); *Oxyrrhis marina* (Om); o indicates that the grazing rates were calculated using *E. huxleyi* k-values from non-grazing controls in experiment 2.

Table 1. Details of experiments performed.

	Experimental Conditions						Parameters Measured (Om)			
	EhV: Eh ratio	**% infected Eh cells 6 h p.i.**	**Eh:Om ratio**	**Initial Om (cells/ml)**	**Vol (ml)**	**Duration (days)**	**Growth Rate**	**Grazing Rate**	**Fatty Acids**	**Cell Vol**
Experiment 1	100:1	30	30:1	6000	50	0.25		x		
Experiment 2	100:1	30	100:1	4500	150	3	x	x	X	
Experiment 3	100:1	30	100:1	4000	150	7	x	o		
Experiment 4	50:1	36	100:1	6000	150	5	x	x		x

Emiliania huxleyi (Eh); *Oxyrrhis marina* (Om); o indicates that the grazing rates were calculated using *E. huxleyi* k-values from non-grazing controls in experiment 2.

Table 2(on next page)

Table 2. Percentage (%) of individual fatty acids to total FA concentration

Percentage (%) of individual fatty acids to total FA concentration of cultures in which: i) *O. marina* was depleted of prey at the start of the experiments (Day 0 Om); ii) the *E. huxleyi* cultures fed to *O. marina*; iii) after three days fed non-infected *E. huxleyi* (Om + Eh non-inf); and iv) after 3 days fed infected *E. huxleyi* (Om +Eh inf). Values are mean ± one standard deviation, n = 4, n = 4, n = 3 and n = 3, respectively. Note the values for *E. huxleyi* are the average of duplicate non-infected and duplicate infected cultures. Significant differences in the proportions of individual compounds are shown as: [a] Day 0 Om vs. *E.huxleyi*; [b] Day 0 Om vs. Day 3 Om + Eh non-inf; [c] Day 0 Om vs. Day 3 Om + Eh inf; and [d] Day 0 Om vs. Day 3 Om + Eh non-inf vs. Day 0 Om vs. Day 3 Om + Eh inf.

Table 2. Percentage (%) of individual fatty acids to total FA concentration of cultures in which: i) *O. marina* was depleted of prey at the start of the experiments (Day 0 Om); ii) the *E. huxleyi* cultures fed to *O. marina*; iii) after three days fed non-infected *E. huxleyi* (Om + Eh non-inf); and iv) after 3 days fed infected *E. huxleyi* (Om +Eh inf). Values are mean ± one standard deviation, n = 4, n = 4, n = 3 and n = 3, respectively. Note the values for *E. huxleyi* are the average of duplicate non-infected and duplicate infected cultures. Significant differences in the proportions of individual compounds are shown as: [a] Day 0 Om vs. *E.huxleyi*; [b] Day 0 Om vs. Day 3 Om + Eh non-inf; [c] Day 0 Om vs. Day 3 Om + Eh inf; and [d] Day 0 Om vs. Day 3 Om + Eh non-inf vs. Day 0 Om vs. Day 3 Om + Eh inf.

FA Class		Day 0 Om	*E. huxleyi*	Day 3 Om + Eh non-inf	Day 3 Om + Eh inf
SFA	**C14:0**	0.2 ± 0.2	0.2 ± 0.1	0.4 ± 0.1	1.2 ± 1.3
	C15:0	0.4 ± 0.3	0.3 ± 0.2	0.5 ± 0.0	0.8 ± 0.4
	C16:0	30.9 ± 4.5	27.6 ± 3.6	29.4 ± 7.6	24.6 ± 2.6
	C17:0	2.7 ± 0.1	2.7 ± 0.7	2.7 ± 0.3	3.2 ± 0.1 [c, d]
	C18:0	36.2 ± 11.1	60.9 ± 7.6 [a]	46.9 ± 6.4	56.4 ± 7.1 [c]
	C20:0	1.1 ± 0.1	1.3 ± 0.3	1.5 ± 0.8	1.2 ± 0.4
	C22:0	0.8 ± 0.2	0.7 ± 0.6	3.3 ± 2.3	1.8 ± 0.9
	C24:0	0.7 ± 0.5	1.1 ± 0.1	0.6 ± 0.4	0.4 ± 0.3
MUFA	**C16:1**	0.8 ± 1.6	0.0	0.0	0.0
	C18:1(n-9cis)	5.0 ± 4.0	0.0 [a]	1.6 ±1.4 [b]	1.6 ± 1.6 [c]
	C18:1(n-9trans)	4.6 ± 3.3	0.0 [a]	1.7 ± 1.5	1.3 ± 1.2
	C22:1	1.1 ± 0.9	0.1 ± 0.1	0.0	0.0
PUFA	**C18:2**	2.7 ± 1.4	0.0	0.0 [b]	0.2 ± 0.3 [c]
	C20:2	2.9 ± 2.3	5.0 ± 3.7	7.1 ± 1.9 [b]	3.2 ± 1.3 [c, d]
	C20:5 (n-3)	1.2 ± 1.2	0.1 ± 0.1	0.2 ± 0.3	0.3 ± 0.3
	C22:6 (n-3)	8.6 ± 7.7	0.0	4.0 ± 4.1	3.9 ± 3.3
	∑ SFA	73 ± 15	95 ± 4 [a]	86 ± 9	89 ± 6
	∑ MUFA	12 ± 8	0.1 ± 0.1 [a]	3 ± 3	3 ± 3
	∑ PUFA	15 ± 8	5 ± 4	11 ± 6	8 ± 3

Table 3(on next page)

Table 3. Cell volumes (µm^3) of *O. marina* fed non-infected and infected *E. huxleyi* over three days during experiment 4.

Oxyrrhis marina (Om); prey-depleted (prey-depl), i.e., not fed for three days; *Emiliania huxleyi* non-infected (Eh non-inf); *Emiliania huxleyi* infected with EhV-86 (Eh inf). Values are mean ± one standard deviation.

Table 3. Cell volumes (µm^3) of *O. marina* fed non-infected and infected *E. huxleyi* over three days during experiment 4.

Treatment	Day	Replicate	Volume (µm^3)
Om prey-depl	0		5586 ± 917
Om + Eh non-inf	1	A	4723 ± 1535
		B	5759 ± 1123
		C	5696 ± 1842
	2	A	4107 ± 1689
		B	3801 ± 660
		C	5602 ± 1045
	3	A	4675 ± 1141
		B	4038 ± 1319
		C	3949 ± 977
Om + Eh inf	1	A	5004 ± 1245
		B	4286 ± 1053
		C	4829 ± 1435
	2	A	6105 ± 462
		B	5561 ± 1483
		C	6977 ± 1371
	3	A	4267 ± 1218
		B	4478 ± 1184
		C	5527± 1956

Oxyrrhis marina (Om); prey-depleted (prey-depl), i.e., not fed for three days; *Emiliania huxleyi* non-infected (Eh non-inf); *Emiliania huxleyi* infected with EhV-86 (Eh inf). Values are mean ± one standard deviation.